

MIT Open Access Articles

Transnuclear TRP1-Specific CD8 T Cells with High or Low Affinity TCRs Show Equivalent Antitumor Activity

The MIT Faculty has made this article openly available. **Please share** how this access benefits you. Your story matters.

Citation: Dougan, S. K. et al. "Transnuclear TRP1-Specific CD8 T Cells with High or Low Affinity TCRs Show Equivalent Antitumor Activity." *Cancer Immunology Research* 1, 2 (July 2013): 99–111
© 2013 American Association for Cancer Research (AACR)

As Published: <http://dx.doi.org/10.1158/2326-6066.CIR-13-0047>

Publisher: American Association for Cancer Research (AACR)

Persistent URL: <http://hdl.handle.net/1721.1/116615>

Version: Author's final manuscript: final author's manuscript post peer review, without publisher's formatting or copy editing

Terms of use: Creative Commons Attribution-Noncommercial-Share Alike





Published in final edited form as:

Cancer Immunol Res. 2013 August ; 1: 99–111. doi:10.1158/2326-6066.CIR-13-0047.

Transnuclear TRP1-specific CD8 T cells with high or low affinity TCRs show equivalent anti-tumor activity

Stephanie K. Dougan¹, Michael Dougan^{1,2}, Jun Kim^{1,3}, Jacob A. Turner^{1,4}, Souichi Ogata^{1,5}, Hyun-Il Cho⁶, Rudolf Jaenisch¹, Esteban Celis⁶, and Hidde L. Ploegh¹

¹Whitehead Institute for Biomedical Research, 9 Cambridge Center, Cambridge, MA 02142

²Department of Medicine, Massachusetts General Hospital, Boston, MA

³Massachusetts Institute of Technology, Cambridge, MA

⁴University of Cincinnati, 2600 Clifton Ave, Cincinnati, OH 45221

⁵Janssen Research and Development, division of Janssen Pharmaceutica NV, Turnhoutseweg 30, Beerse B2340, Belgium

⁶Dept. of Immunology, H. Lee Moffitt Cancer Center & Research Institute, 12902 Magnolia Drive, Tampa, FL 33612

Abstract

We have generated, via somatic cell nuclear transfer, two independent lines of transnuclear (TN) mice, using as nuclear donors CD8 T cells, sorted by tetramer staining, that recognize the endogenous melanoma antigen TRP1. These two lines of nominally identical specificity differ greatly in their affinity for antigen (TRP1^{high} or TRP1^{low}) as inferred from tetramer dissociation and peptide responsiveness. Ex vivo-activated CD8 T cells from either TRP1^{high} or TRP1^{low} mice show cytolytic activity in 3D tissue culture and *in vivo*, and slow the progression of subcutaneous B16 melanoma. Although naïve TRP1^{low} CD8 T cells do not affect tumor growth, upon activation these cells function indistinguishably from TRP1^{high} cells *in vivo*, limiting tumor cell growth and increasing mouse survival. The anti-tumor effect of both TRP1^{high} and TRP1^{low} CD8 T cells is enhanced in RAG-deficient hosts. However, tumor outgrowth eventually occurs, likely due to T cell exhaustion. The TRP1 TN mice are an excellent model for examining the functional attributes of T cells conferred by TCR affinity, and they may serve as a platform for screening immunomodulatory cancer therapies.

Keywords

melanoma; B16; T cell receptor; somatic cell nuclear transfer; tyrosinase related protein 1

Introduction

Infiltration of CD8 T cells correlates positively with patient outcomes, as shown for colorectal and other cancers (1, 2). Even in the absence of a successful endogenous anti-

Corresponding author: Hidde L. Ploegh, Whitehead Institute, 9 Cambridge Center, Rm 361, Cambridge, MA 02142, Phone: (617) 324-2031, Fax: (617) 452-3566, ploegh@wi.mit.edu.

Conflict of interest: SO is an employee of Janssen Pharmaceuticals. The authors have no other conflicts of interest to disclose.

Online supplementary material: TCR α and TCR β sequences from TRP1^{high} and TRP1^{low} mouse lines were determined by 5'RACE of cDNA from purified CD8 T cells. Figure S1 shows annotated sequences and analysis against the IMGT database ("IMGT", the international ImMunoGeneTics information system@ <http://www.imgt.org>).

tumor immune response, immunotherapy for cancer has begun to deliver on its promise (3, 4). The success of checkpoint blockade therapies such as anti-CTLA-4 illustrates the importance of the CD8 T cell response in tumor regression. At baseline, many human cancer patients have anti-tumor CD8 T cells that are anergic or kept in check by regulatory CD4 T cells (Tregs). CTLA-4 blockade can activate anti-tumor T cells and elicit clinical responses in 25% of patients. Anti-CTLA-4 works synergistically with chemotherapy, radiation, or other therapies that generate tumor lysis and uptake of tumor antigens by dendritic cells (5). Blocking antibodies to PD-1 and PDL1 (6, 7) produce similar outcomes. The endogenous T cell response to tumors correlates with overall survival in cancer patients (1), and therapies aimed at boosting the T cell response are now in widespread use (3, 8).

Many tumor antigens are mutated self antigens or antigens that are over-expressed. TCRs on T cells that recognize such antigens are generally of low affinity (9) since high-affinity self-reactive cells are deleted in the thymus (10, 11) and suppressed in the tumor microenvironment (12). The type of CD8 T cell response necessary for optimal tumor rejection remains poorly characterized due to a paucity of animal models. Most of the available animal models make use of TCR transgenic animals, the construction of which is based on long term T cell cultures from which the corresponding rearranged TCR segments are cloned and expressed as transgenes. Alternatively, tumor cell lines are engineered to express antigens for which TCR transgenics happen to be available. By their very nature, populations of T cells harvested from tumor-bearing animals or tumor-infiltrating lymphocytes are necessarily heterogeneous, polyclonal and variable from one experiment to the next, exactly the reason why TCR transgenics are so widely used. Models of anti-tumor immunity typically rely on overexpression of ovalbumin in combination with OTI transgenic T cells, known to be of very high affinity. Pmel TCR transgenic mice contain CD8 T cells of more moderate affinity for the endogenous melanoma antigen tyrosinase related protein 1 (TRP1), but results from these mice are difficult to compare to ovalbumin/OTI systems due to differences in the antigen.

Somatic cell nuclear transfer may be used to clone mice from the nuclei of antigen-specific lymphocytes (13–16). These transnuclear mice are derived from primary CD8 T cells harvested in the course of a natural immune response, without any prolonged tissue culture to select for high affinity T cell variants *in vitro*. TN mice contain no genetic alterations other than the rearranged TCR genes, expressed from their endogenous loci and under physiological control. Finally, creation of TN mice can be done rapidly, requiring only 6 weeks from isolation of a selected lymphocyte population, accomplished through isolation of Class I MHC-tetramer positive cells, to birth of chimeric mice. A key advantage of the transnuclear technology is the ability to clone multiple lines of mice with the same antigenic specificity but with different TCR sequences and therefore different affinities (15). These mice can then be used as a ready source of lymphocytes of defined specificity for *in vitro* culture or for adoptive transfer experiments.

Most tumors are weakly immunogenic at best. The well-studied melanoma cell line B16 downregulates Class I MHC and is poorly infiltrated by immune cells (17–19). CD8+ T cells can reject B16 *in vivo*, but only when mice are first exposed to some form of immune manipulation, such as vaccination with irradiated B16, engineered to secrete the cytokine GM-CSF (18, 20, 21). Since B16 does not induce a detectable CD8+ T cell response under normal conditions, we used a peptide-based vaccine strategy to elicit a robust CD8+ T cell response to the melanoma-specific antigen tyrosinase-related protein 1 (TRP-1). This vaccine consists of a palmitoylated version of the peptide to increase its circulatory half-life, anti-CD40 antibody, and the TLR3 ligand polyinosine-polycytidylic acid (poly-IC) and is referred to as TRIVAX. When administered to mice, it elicits a robust population of tetramer + CD8+ T cells that can reject established B16 tumors (22, 23).

We have used such vaccine-induced CD8 T cells as a source of donor nuclei to generate two independent lines of TRP1-specific transnuclear mice. In so doing, we have generated, for the first time, a pair of transnuclear mice with TCRs specific for the identical peptide-MHC combination. These TCRs are expressed under the control of their endogenous promoters and represent cells directly harvested from an immunized mouse upon staining with the appropriate Class I MHC tetramers, without pre-selection in tissue culture, and differ in their affinity for TRP1 by approximately 100-fold. The T cells from these mice recognize an endogenous tumor antigen and allow a direct assessment of the role of TCR affinity in anti-tumor CD8 T cell responses. The generation of anti-tumor TN mice provides a unique set of tools for the fields of tumor immunology and CD8 T cell development.

Materials and Methods

Animal care

All animals were housed at the Whitehead Institute for Biomedical Research and were maintained according to protocols approved by the MIT Committee on Animal Care. C57Bl/6, CD45.1 congenics, and OT-I transgenic mice were purchased from Jackson Labs. RAG2^{-/-} (RAG2TN12) mice were purchased from Taconic.

TN mouse generation

TN mice were generated as previously described (14,15, 24). Briefly, CD8⁺ TRP1 tetramer⁺ cells were sorted by FACS and used as a source of donor nuclei for SCNT. The mitotic spindle was removed from mouse oocytes and replaced with donor nuclei. The nucleus-transplanted oocytes were then activated in medium containing strontium and TSA, and allowed to develop in culture to the blastocyst stage. Because the live birth rate of SCNT blastocysts is close to zero, SCNT blastocysts were instead used to derive embryonic stem (ES) cell lines. These ES cell lines were then injected into wild type B6xDBA F1 blastocysts and implanted into pseudopregnant females. The resulting chimeric pups were mated to C57Bl/6 females to establish the 6.15 (TRP1^{low}) and 6.17 (TRP1^{high}) lines. All animals used were backcrossed 4–7 generations onto the C57BL/6 background.

Sequencing of the TCR genes

TRP1^{high} and TRP1^{low} CD8 T cells were purified by positive selection using CD8 magnetic beads (Miltenyi Biotec) and used as a source of RNA. 5'RACE was performed according to the manufacturer's protocol (GeneRacer, #L1502-01 Invitrogen).

MHC tetramer production and peptide exchange

Recombinant protein expression, refolding of the H-2D^b complex with the SV9-P7* conditional ligand, and their subsequent tetramerization were accomplished by following established protocols (25–27). The peptide exchange reaction was initiated by UV irradiation (360 nm), and the resulting MHC tetramers were used directly to stain freshly prepared splenocytes as described previously. TRP1 altered peptide ligands were produced by Fmoc-based solid-phase peptide synthesis by the MIT Center for Cancer Research (Cambridge, MA) biopolymers facility. All peptides were dissolved in dimethyl sulfoxide (10 mg/ml) and stored at –20°C until further use.

Flow cytometry

Cells were harvested from spleen, peripheral blood or thymus. Cell preparations were subjected to hypotonic lysis to remove erythrocytes, stained and analyzed using a FACSCalibur (BD). Tetramers were prepared fresh from photocleavable stocks (25–27) or

directly refolded with TRP1 heteroclytic peptide (TAPDNLGYM). All antibodies were from BD Pharmingen.

Cell culturing

Cells were cultured in RPMI 1640 medium supplemented with 10% heat-inactivated FBS, 2 mM l-glutamine, 100 U/ml penicillin G sodium, 100 µg/ml streptomycin sulfate, 1 mM sodium pyruvate, 0.1 mM nonessential amino acids, and 0.1 mM 2-ME. Bone marrow-derived dendritic cells were obtained by culturing of bone marrow aspirates in RPMI media supplemented with rmGM-CSF (Peprotech) and rmIL-4 (Peprotech). Fresh media was added to the BMDC cultures every 2 days for 6 days. BMDCs were used at day 6–8 of differentiation, and were washed prior to use. CD8 T cells were isolated from pooled spleen and LNs of TRP1 TN or wild type mice using positive selection on anti-CD8 magnetic beads (Dynabeads, Invitrogen). For cocultures, BMDCs were pulsed with the indicated peptides for 30 minutes prior to the addition of CD8 T cells at a ratio of 100,000 T cells to 50,000 BMDCs in round-bottom 96 well culture plates. IL-2 and IFN- γ production were measured by ELISA of 24, 48 or 72 hour culture supernatants as indicated (BD Pharmingen). RANTES and MIP-1 β were measured by cytokine bead array (BD).

3D B16 tumor cultures

CD8 T cells from TRP1^{high}, TRP1^{low} or OT-I transgenic mice were isolated by positive selection on anti-CD8 Dynabeads (Invitrogen, 114.62D) and cultured for 18 hours with BMDCs plus either TRP1 heteroclytic peptide or OVA peptide (SIINFEKL) at 1 µM concentration. Activated CD8 cells were then counted mixed with B16 cells at 20:1 ratio and resuspended in 3-D culture matrix cocktail as follows: D-PBS containing 33% of Cultrex BME (Trevigen 3445-005-01), 10% FCS, 1 mg/ml Fibrinogen (Calbiochem, 341578), 1.4 U/mL Thrombin (MP Biomedicals, 02194083), 1.25×10⁵ cells/mL of B16 and 2.5×10⁶ or 5.0×10⁶ cells/mL of CD8⁺ T-cells. 55 µl of this cell+matrix cocktail was cast in flat bottom 96 well plates, incubated for 45 minutes to allow the matrix become solid and then overlaid with 100 µl of DMEM+10% FCS medium on top of the solid gel matrix. Cultures were incubated for 4 days. Cells were reisolated in ice-cold PBS+5mM EDTA, washed, and resuspended in PBS+0.5% BSA and stained using anti-CD8 and the viability dye 7-AAD (BD Pharmingen). B16 cells were quantified as a ratio of 7-AAD⁺ to 7-AAD⁻ cells to determine the dead:live ratio.

B16 tumor inoculations

B16 cells were a kind gift of Dr. Glenn Dranoff (Dana Farber Cancer Institute, Boston, MA). B16 cells were cultured to 90% confluency, trypsinized, washed in HBSS and resuspended in HBSS at 50,000 tumor cells per 250 µL volume. Cells were injected subcutaneously in the left flank of 6–12 week old female C57BL/6 mice. In mice receiving no transferred T cells, palpable tumors arose 7–10 days post-inoculation. Tumor diameter was measured in 3 dimensions, and mice were sacrificed when tumor volume reached 2 cubic cm. For adoptive transfers, unless otherwise stated, mice received 300,000 CD8 T cells in 150 µL PBS administered via tail vein injection within 24 hours of tumor inoculation.

Statistics

Statistical analysis of survival curves was performed using GraphPad Prism software. p values were determined using the Mantel-Cox log rank test. Delays in tumor growth were obtained by comparison of median survival times.

Results

Generation of high and low affinity TRP1 TN mice

Vaccination with palmitoylated TRP-1 peptide, anti-CD40 antibody, and the TLR3 ligand polyinosine-polycytidylic acid (poly-IC) yields a robust population of anti-TRP-1 CD8⁺ T cells relatively quickly and provides a source of TRP-1 specific lymphocytes for SCNT. SCNT is most successful using hybrid mouse strains as a source of donor nuclei. To this end, B6x129 F1 male agouti mice were injected intravenously with palmitoylated peptide TAPDNLGYM, anti-CD40 and poly-IC. The TRP1 peptide sequence used differs from native TRP1 in the 9th position (A to M substitution) to increase its binding to H-2D^b. This heteroclitic peptide was used to construct TRP1 tetramers, and robust TRP-1 tetramer positive populations were observed in the spleens of immunized mice at 6 and 8 days post-immunization (Figure 1A). These CD8⁺ TRP-1 tetramer⁺ populations were sorted by FACS and used as a source of donor nuclei for two separate SCNT experiments. A total of 105 nuclear transfers were performed, yielding 5 independent ES cell lines (Figure 1B). Of these, two resulted in agouti chimeric mice containing TRP-1 tetramer⁺ CD8⁺ T cells in peripheral blood (Figure 1C).

Both lines of TRP1 transnuclear mice gave germline transmission, and the F1 progeny showed skewing of the CD4:CD8 ratio, with a large percentage of TRP1 tetramer⁺ cells at baseline (Fig 1D). Tetramer⁺ CD8 T cells were sorted from each mouse line and subjected to 5'RACE to sequence the TCR α and TCR β genes (Supplemental Figure 1). The 6.15 mice had consistently fewer TRP1 tetramer⁺ cells than their 6.17 counterparts, and the tetramer staining was dimmer, as judged by a reduction in mean fluorescent intensity. TCR, CD3 and CD8 surface expression were normal on 6.15 cells (data not shown), so we hypothesized that the lower intensity tetramer staining was due to weaker binding of tetramers to the TCR. To measure TCR avidity, splenocytes from 6.15 or 6.17 mice were incubated with TRP1 tetramer at saturating conditions, washed, and incubated for various periods of time to allow dissociation of the TCR-peptide-MHC complexes (Figures 2A and 2B). 6.15 cells rapidly lost tetramer staining, such that by 30 minutes all cells were tetramer-negative and indistinguishable from background. 6.17 cells lost fluorescence over time, but a significant fraction remained tetramer-positive even after overnight incubation. Thus, CD8 T cells from 6.17 mice show slower tetramer dissociation than do 6.15 cells ($t_{1/2}$ = 41 min vs. 4.9 min); we therefore reclassified these TN mouse lines as TRP1^{high} and TRP1^{low}, respectively.

The degree to which cultured CD8 T cells can produce cytokines in response to properly presented serial dilutions of peptide correlates with anti-tumor function (28). We cultured isolated CD8 T cells from TRP1 TN mice with bone marrow-derived DCs (BMDCs) pulsed with different amounts of TRP1 peptide, either the heteroclitic variant used for tetramer staining or the native TRP1 sequence. TRP1^{low} T cells were unable to respond to the heteroclitic TRP1 peptide at concentrations less than 100 pg/mL while TRP1^{high} T cells secreted IFN- γ in response to as little as 1 pg/mL peptide under the same conditions (Figure 2C). Both TRP1^{high} and TRP1^{low} cells produced IFN- γ in response to native TRP1 peptide, but higher concentrations of peptide were required (Figure 2D). In addition to IFN- γ , we also measured chemokine production. TRP1^{low} cells produced RANTES and MIP1- α even when exposed to concentrations of peptide (Figure 2E) that yielded negligible IL-2 or IFN- γ production, confirming previous studies showing a hierarchy of effector functions based on TCR affinity (29).

TRP altered peptide ligands assess fine specificity of TCR

A panel of TRP1 altered peptide variants was generated (Figure 3A) that differed from the heteroclitic reference peptide by single amino acid substitutions. No substitutions were made

in anchor residue positions. Sorted CD8 cells from TRP1^{high} and TRP1^{low} mice were incubated with BMDCs pulsed with the altered peptide ligands to assess IL-2 and IFN- γ production (Figure 3B). TRP1^{high} T cells were more promiscuous than TRP1^{low} T cells. One peptide (A1) generated similar levels of both IL-2 and IFN- γ from both TRP1^{high} and TRP1^{low} CD8 cells, demonstrating that the lower cytokine production typically observed from cells from TRP1^{low} mice is not an intrinsic limit on the ability of these cells to produce cytokine.

Minor differences between TRP1^{high} and TRP1^{low} cells during thymic development and in the naïve state

We compared the surface profile of naïve CD8 cells from age-matched TRP1 TN mice and found that TRP1^{low} cells show higher expression of NK1.1 and KLRG1 than TRP1^{high} or wild type control cells (Figure 4A). No differences were seen in Tim3 or CD25 staining, suggesting that NK receptor upregulation is not a function of global activation state, but rather an intrinsic difference established by the clonotypic T cell receptors.

CD5 expression correlates with intensity of TCR signaling and is tightly regulated during T cell development (30). TRP1^{low} cells also expressed lower levels of CD5 in both the periphery and during thymic development, while TRP1^{high} cells showed a curious peak of CD5 expression in CD4+CD8+ thymocytes (Figure 4B). TRP1^{high} cells show a decrease in CD4+CD8+ thymocytes and an increase in TCR β and CD3 ϵ expression at the CD4+CD8+ stage, indicative of accelerated thymic development, as is typical of mice with pre-rearranged TCR genes. TRP1^{low} cells did not show accelerated thymic development. Overall, thymic development in both TRP1 TN mouse strains is near-normal, and the T cells produced have a naïve phenotype.

TRP1 TN CD8 T cells are cytotoxic *in vitro*

To determine whether TRP1 cells could be cytotoxic, we activated TRP1^{high} and TRP1^{low} CD8 T cells with anti-CD3/CD28 coated beads for 7 days and cultured with TRP1 A1 peptide-pulsed GFP+ B cells mixed with unlabeled B cells at a 1:1 ratio. Both high and low affinity TRP1 cells displayed specific killing in a dose-dependent fashion, with TRP1^{low} cells slightly outperforming TRP1^{high} cells (Figure 5A). To determine whether TRP1 TN cells could exert cytotoxic function against tumor cells, we established 3D cocultures using B16 cells and CD8 T cells seeded together in Matrigel. B16, whether grown in culture or explanted from a mouse, expresses TRP1 protein as evidenced by immunoblotting (Figure 5B). Coculture of B16 and TRP1 TN cells showed an increase in the ratio of dead/live tumor cells in groups that received either TRP1^{low} or TRP1^{high} CD8 T cells. These results show that both lines of TRP1 TN cells can be cytotoxic under 3D culture conditions (Figure 5C). Again, TRP1^{low} cells tended to show greater cytotoxicity than TRP1^{high} cells although these differences did not reach statistical significance.

TRP1 TN cells delay tumor growth *in vivo*

To assess their tumor-protective function *in vivo*, naïve CD8 T cells isolated from TRP1^{high} or TRP1^{low} mice were transferred into wild type recipients simultaneously with subcutaneous inoculation with B16 melanoma. The B16 dose of 50,000 cells was empirically determined such that tumors would first become palpable at day 7–10 post-inoculation and 50% of untreated mice would require euthanasia by 21 days post-inoculation. Under these conditions, administration of naïve TRP1^{high} cells showed a modest 2 day difference in median survival while TRP1^{low} cells had no discernible effect on tumor growth (Figure 6A). Administration of multiple doses of naïve CD8 T cells (at days 0, 3, and 5 post tumor inoculation) gave similar results to single dose trials, with TRP1^{high}

cells conferring a 2 day survival benefit and TRP1^{low} cells having no discernible effect (data not shown).

We next analyzed the effect of *ex vivo* activation of the TRP1 cells prior to adoptive transfer. CD8 T cells from TRP1^{high} or TRP1^{low} mice were cultured with BMDCs and TRP1 peptide for 18 hours and transferred into wild type hosts at day 1 post-inoculation with B16. Under these conditions, both TRP1^{high} and TRP1^{low} cells conferred a 4 day increase in mean survival (Figure 6B). Thus TRP1^{low} cells acquire anti-tumor properties equal to their high affinity counterparts upon *ex vivo* activation. As further confirmation, CD8 T cells from the same TRP1^{low} donor mouse were adoptively transferred either naïve, or after culture with peptide-pulsed BMDCs (Figure 6C). Although activation of polyclonal CD8 T cells has a modest effect, possibly due to the selective expansion of TRP1-specific cells from the polyclonal pool, activated TRP1^{low} cells conferred an additional 5 day increase in median survival when compared to polyclonal activated CD8 T cells (Figure 6C).

Studies using transgenic CD8 T cells from Pmel mice have shown that decreasing the number of transferred CD8 T cells leads to increased proliferation rates and increased anti-tumor effects of the transferred cells (31). In Figures 6A–C, we administered a constant dose of 3 million TRP1 cells per mouse. Peptide-activated TRP1^{high} cells retained their anti-tumor activity at lower doses, and showed optimal anti-tumor effect at a dose of 300,000–500,000 cells (Figure 6D); the 300,000 T cell dose was used for all subsequent experiments. To assess possible synergy between TRP1^{high} and TRP1^{low} cells, purified CD8 T cells from each TN mouse line were peptide-activated *ex vivo* and transferred into wild type hosts, either alone or mixed at a 1:1 ratio. The total number of transferred T cells remained constant. The combination of TRP1^{high} plus TRP1^{low} cells did not confer additional survival benefit beyond what could be seen with either population alone (Figure 6E).

The cumulative effect of activated TRP1 TN cells against subcutaneous B16 caused a delay, but did not prevent tumor growth. This eventual failure to control the tumor could be due to several factors: 1) incomplete activation of the TRP1 TN cells *ex vivo*; 2) failure to traffic to the tumor; 3) immunosuppression in the tumor microenvironment; or 4) loss of the TRP1 epitope. To address some of these issues, we first cultured TRP1^{high} cells with anti-CD3/CD28 coated beads and found that 40% of mice survived (Figure 6F). We next transferred naïve TRP1^{high} or TRP1^{low} cells into RAG-deficient mice to induce homeostatic proliferation of the transferred T cells and to observe TRP1 TN CD8 T cell function in the absence of CD4⁺ Tregs. When challenged with B16, the RAG-deficient mice reconstituted with either TRP1^{high} or TRP1^{low} cells showed a 7 day delay in tumor growth (Figure 7A). The tumors harvested from RAG-deficient mice in Figure 7 were melanotic, showing that melanin production was intact. Immunoblotting for TRP1 protein showed no decrease in overall TRP1 levels (data not shown). A more likely explanation for the eventual failure of CD8 T cells to control tumor growth is exhaustion. In RAG-deficient hosts, which lack endogenous T cells, the tumor infiltrating CD8 T cells are derived entirely from the transferred TRP1 TN population. Both TRP1^{high} and TRP1^{low} cells can migrate to the tumor, yet even when they accumulate to the extent seen in RAG-deficient hosts, they eventually fail to control tumor outgrowth. Surface expression of PD-1 and LAG3 was increased on TRP1 TN cells harvested from end-stage tumors (Figure 7B), consistent with exhaustion (32, 33).

Discussion

The role of TCR affinity in the anti-tumor T cell response remains a topic of debate. On the one hand, the endogenous pool of anti-tumor T cells is generally low affinity, presumably because T cells bearing high affinity TCRs that might recognize antigens on tumors are

deleted in the course of thymic development, as most such antigens represent self-antigens expressed at supranormal levels. Tumor-specific CD8 T cells express TCRs of much lower affinity than typical anti-viral T cells, as was recently quantified for 24 different human TCRs (9). The repertoire of anti-tumor TCRs is limited not only by thymic deletion of high-affinity self-reactive clones but also by negative regulatory mechanisms in the tumor environment. However, high affinity anti-tumor T cells can be generated in experimental mouse models or can be expanded by *ex vivo* culturing of human samples. The increased use of chimeric antigen receptors (34, 35), usually selected to display higher affinities for their cognate antigens than those of typical endogenous TCRs, demands a better understanding of these supraphysiologic binding affinities: how does increased TCR affinity affect functional outcomes such as cytokine production, cytotoxicity and memory formation? The role of TCR affinity with respect to tumor destruction and long-term anti-tumor memory is therefore an important question and at a minimum would require the comparison of T cells that recognize the same antigen with different affinities.

Although intuitively the highest affinity T cells would seem to be the most efficacious at tumor regression, the situation is likely more complicated. In human CMV infection, a population of T cells with such low affinity that they fail to bind MHC tetramers still produces more IFN γ and is more cytotoxic than higher affinity T cells from that same individual (36). Several lines of evidence suggest that a CD8 T cell's fate is determined, or programmed, by its initial encounter with antigen (37–39). Duration and strength of antigenic stimulation are inversely correlated with CD8 memory cell differentiation during acute viral infection (38, 39). Low affinity T cells can increase their functional avidity by upregulating expression of CD8. Conversely, high affinity T cells downregulate CD8 expression in order to avoid antigen-induced cell death (39, 40). Upon encountering abundant antigen, high avidity CD8 T cells cease proliferation and initiate apoptosis, although they can still exert cytotoxic function prior to death (18).

Adoptive cell transfer therapy, as pioneered by the Rosenberg group, selects for the highest affinity CD8 T cells and aims for maximal activation *in vitro* prior to infusion into the patient. This strategy has been remarkably successful in a limited clinical population (41–43), and suggests that high affinity, maximally activated CD8 T cells confer the maximal anti-tumor response. Likewise, comparison of two different T cell lines specific for the same model antigen overexpressed in the pancreas showed that the higher affinity Clone 4 cells were better able to expand in the pancreatic environment and cause tumor destruction, as measured by increased serum glucose (44) although low affinity Clone 1 cells were able to mediate tumor destruction when paired with antigen-specific CD4 cells (45). However, when the same Clone 4 cells were injected into mice with HA-expressing renal cell carcinomas, the anti-tumor effects of high affinity Clone 4 cells were curtailed by suppressive mechanisms in the tumor microenvironment (46). Sequence analysis of TCRs from T cells induced by effective versus ineffective vaccine strategies shows that higher affinity T cells were induced by the effective vaccines, although the K_D values measured for each group differed by less than 2-fold (47).

On the other hand, several studies have suggested that an optimal CD8 T cell response uses low to moderate affinity TCRs. Retroviral transduction of T cells with a panel of TCRs of known gradations in affinity showed that the highest affinity TCRs were absent from tumor-infiltrating CD8 T cells, although these TCRs could be found on tumor-infiltrating CD4 cells (48). A panel of NY-ESO1 specific T cell lines engineered to express TCRs with affinities ranging from low to supra-physiological showed that optimal cytotoxicity and calcium flux occurred using TCRs with intermediate K_D values of 1–5 micromolar with a decline in functionality for higher affinity TCRs (49, 50). A similar ceiling was observed using vaccination with peptide mimetics with a range of affinities for a given T cell clone

(51). A recent study evaluated a large panel of human anti-melanoma cell lines for peptide sensitivity, production of various cytokines and TCR affinity as defined by the kinetics of multimer binding. Although peptide sensitivity and production of IL-2, TNF α and IFN- γ correlated with tumor cell killing, multimer binding failed to correlate with any of the functional parameters measured (28), suggesting that TCR affinity alone could not predict anti-tumor responses. This raises the interesting possibility that attributes other than affinity, yet associated with a particular TCR clonotype, may determine the functional property of a T cell. Using tumors transduced with altered peptide ligands for OT-I CD8 T cell recognition, low affinity TCR interactions generated enhanced cytokine production during both primary and secondary responses, but the lower affinity T cells were more susceptible to TGF- β mediated suppression (52). An interesting study compared the TCR affinity of the endogenous CD8 response to ovalbumin-expressing glioma as a function of the vaccine injection site (53). Mice vaccinated at sites proximal to the tumor generated lower affinity CD8 T cells than mice vaccinated at more distant sites, which could implicate suppressive mechanisms that specifically limit high-affinity CD8 priming in the tumor draining lymph nodes (53).

In the TRP1 TN system, we show that an approximately 10-fold difference in tetramer dissociation rates and a 100-fold difference in peptide responsiveness have almost no effect on the overall anti-tumor function of the transferred CD8 T cells. How do the low affinity T cells manage to perform as well as their high affinity counterparts? Although tetramer dissociation and IFN- γ production showed clear distinctions between the two TRP1-specific TN lines, we observed much less of a difference when comparing cytotoxic function in a 3D culture model. Likewise, both TRP1^{high} and TRP1^{low} cells produced the chemokines RANTES and MIP1 α when stimulated with picomolar concentrations of native TRP1 peptide, conditions under which no IL-2 or IFN- γ could be detected in supernatants from the TRP1^{low} cultures. Since the concentration of antigen presented in a tumor-bearing mouse is likely to be small, the fact that TRP1^{low} cells produce monocyte-attracting chemokines in response to low doses of peptide could be relevant for how TRP1^{low} CD8 T cells influence the tumor microenvironment. Likewise, the increased IL-2 production from TRP1^{high} cells could enhance Treg recruitment or proliferation in the tumor microenvironment, although such an effect would be eliminated in RAG-deficient hosts, which lack Tregs. Another likely possibility is increased activation-induced cell death of TRP1^{high} cells in the tumor environment, which could limit the efficacy of high affinity CD8 cells (54, 55). Indeed, TRP1^{high} tumor infiltrating cells show reduced CD8 expression, indicative of a more activated state.

Here we have generated a pair of mice with T cells specific for the same MHC-peptide combination but differing in affinity by one to two orders of magnitude. The TCR α and β chains are under the control of their endogenous promoters, and expressed at physiological levels. Both TCRs were selected by directly harvesting tetramer+ CD8 cells from a vaccinated mouse without any selection in tissue culture, and thus are representative of the normal pool of activated CD8 T cells that arises during an immune response. As such, we anticipate that the TRP1 TN mice reported here may be useful for studies of T cell development and T cell activation.

Although TRP1 is a self-antigen expressed in healthy melanocytes, we did not observe vitiligo in TRP1^{high} or TRP1^{low} mice on a RAG-proficient background, suggesting a possible role for CD4+ regulatory T cells. Tregs are absent in TRP1^{high} RAG2^{-/-} mice, and these mice develop a mild spontaneous vitiligo around 3 months of age, affecting primarily the periorbital region. The Tregs that develop in TRP1 TN mice are constrained to using a single TCR V β 8.2 or TCR V β 5 respectively, thus limiting the diversity of potential Tregs

specificities in these mice. Nevertheless, the Tregs that develop are apparently adequate to prevent autoimmunity even in the presence of a high fraction of autoreactive CD8 T cells.

TRP1 can serve as a tumor rejection antigen, and we show a modest anti-tumor effect of anti-TRP1 CD8 T cells as a monotherapy. Although the effects are small, the delay in tumor growth and slight increase in overall survival parallels the human situation, where monotherapies such as anti-CTLA-4 also show modest clinical benefit (56). A future challenge for tumor immunology will be to determine which therapies synergize in order to achieve maximum clinical effect. CD8 T cell exhaustion is commonly observed in human patients, and must be overcome in order for immunotherapy to succeed. The TRP1 mice offer an excellent pre-clinical platform for testing the immune modulatory effects of potential new drugs or drug combinations.

Supplementary Material

Refer to Web version on PubMed Central for supplementary material.

Acknowledgments

We are grateful to Patti Wisniewski and Chad Araneo for cell sorting, and to John Jackson for mouse husbandry.

Grant support

SKD was funded by the Cancer Research Institute and by the Bushrod H. Campbell and Adah F. Hall Charity Fund and Harold Whitworth Pierce Charitable Trust. SO was funded by Janssen Pharmaceutica NV. EC, HLP and RJ are funded by grants from the NIH. SKD and HLP are funded by Janssen Pharmaceuticals, Inc and by the AACR-Pancreatic Cancer Action Network.

References

1. Galon J, Costes A, Sanchez-Cabo F, Kirilovsky A, Mlecnik B, Lagorce-Pages C, et al. Type, density, and location of immune cells within human colorectal tumors predict clinical outcome. *Science*. 2006; 313(5795):1960–4. [PubMed: 17008531]
2. Hodi FS, Butler M, Oble DA, Seiden MV, Haluska FG, Kruse A, et al. Immunologic and clinical effects of antibody blockade of cytotoxic T lymphocyte-associated antigen 4 in previously vaccinated cancer patients. *Proc Natl Acad Sci U S A*. 2008; 105(8):3005–10. [PubMed: 18287062]
3. Dougan M, Dranoff G. Immune therapy for cancer. *Annu Rev Immunol*. 2009; 27:83–117. [PubMed: 19007331]
4. Hodi FS, O'Day SJ, McDermott DF, Weber RW, Sosman JA, Haanen JB, et al. Improved survival with ipilimumab in patients with metastatic melanoma. *N Engl J Med*. 2010; 363(8):711–23. [PubMed: 20525992]
5. Korman AJ, Peggs KS, Allison JP. Checkpoint blockade in cancer immunotherapy. *Adv Immunol*. 2006; 90:297–339. [PubMed: 16730267]
6. Brahmer JR, Tykodi SS, Chow LQ, Hwu WJ, Topalian SL, Hwu P, et al. Safety and activity of anti-PD-L1 antibody in patients with advanced cancer. *N Engl J Med*. 2012; 366(26):2455–65. [PubMed: 22658128]
7. Topalian SL, Hodi FS, Brahmer JR, Gettinger SN, Smith DC, McDermott DF, et al. Safety, activity, and immune correlates of anti-PD-1 antibody in cancer. *N Engl J Med*. 2012; 366(26):2443–54. [PubMed: 22658127]
8. Pardoll DM. The blockade of immune checkpoints in cancer immunotherapy. *Nat Rev Cancer*. 2012; 12(4):252–64. [PubMed: 22437870]
9. Aleksic M, Liddy N, Molloy PE, Pumphrey N, Vuidepot A, Chang KM, et al. Different affinity windows for virus and cancer-specific T-cell receptors: Implications for therapeutic strategies. *Eur J Immunol*. 2012; 42(12):3174–9. [PubMed: 22949370]

10. Bouneaud C, Kourilsky P, Bousso P. Impact of negative selection on the T cell repertoire reactive to a self-peptide: a large fraction of T cell clones escapes clonal deletion. *Immunity*. 2000; 13(6): 829–40. [PubMed: 11163198]
11. Nugent CT, Morgan DJ, Biggs JA, Ko A, Pilip IM, Pamer EG, et al. Characterization of CD8+ T lymphocytes that persist after peripheral tolerance to a self antigen expressed in the pancreas. *J Immunol*. 2000; 164(1):191–200. [PubMed: 10605011]
12. Willimsky G, Blankenstein T. Sporadic immunogenic tumours avoid destruction by inducing T-cell tolerance. *Nature*. 2005; 437(7055):141–6. [PubMed: 16136144]
13. Dougan SK, Ogata S, Hu CC, Grotenbreg GM, Guillen E, Jaenisch R, et al. IgG1+ ovalbumin-specific B-cell transnuclear mice show class switch recombination in rare allelically included B cells. *Proc Natl Acad Sci U S A*. 2012; 109(34):13739–44. [PubMed: 22869725]
14. Kirak O, Frickel EM, Grotenbreg GM, Suh H, Jaenisch R, Ploegh HL. Transnuclear mice with predefined T cell receptor specificities against *Toxoplasma gondii* obtained via SCNT. *J Vis Exp*. 2010; (43)
15. Kirak O, Frickel EM, Grotenbreg GM, Suh H, Jaenisch R, Ploegh HL. Transnuclear mice with predefined T cell receptor specificities against *Toxoplasma gondii* obtained via SCNT. *Science*. 2010; 328(5975):243–8. [PubMed: 20378817]
16. Sehrawat S, Kirak O, Koenig PA, Isaacson MK, Marques S, Bozkurt G, et al. CD8(+) T Cells from Mice Transnuclear for a TCR that Recognizes a Single H-2K(b)-Restricted MHV68 Epitope Derived from gB-ORF8 Help Control Infection. *Cell Rep*. 2012; 1(5):461–71. [PubMed: 22832272]
17. Curran MA, Montalvo W, Yagita H, Allison JP. PD-1 and CTLA-4 combination blockade expands infiltrating T cells and reduces regulatory T and myeloid cells within B16 melanoma tumors. *Proc Natl Acad Sci U S A*. 107(9):4275–80. [PubMed: 20160101]
18. Quezada SA, Peggs KS, Curran MA, Allison JP. CTLA4 blockade and GM-CSF combination immunotherapy alters the intratumor balance of effector and regulatory T cells. *J Clin Invest*. 2006; 116(7):1935–45. [PubMed: 16778987]
19. Taniguchi K, Karre K, Klein G. Lung colonization and metastasis by disseminated B16 melanoma cells: H-2 associated control at the level of the host and the tumor cell. *Int J Cancer*. 1985; 36(4): 503–10. [PubMed: 4044058]
20. Dranoff G, Jaffee E, Lazenby A, Golumbek P, Levitsky H, Brose K, et al. Vaccination with irradiated tumor cells engineered to secrete murine granulocyte-macrophage colony-stimulating factor stimulates potent, specific, and long-lasting anti-tumor immunity. *Proc Natl Acad Sci U S A*. 1993; 90(8):3539–43. [PubMed: 8097319]
21. Dougan M, Dougan S, Slisz J, Firestone B, Vanneman M, Draganov D, et al. IAP inhibitors enhance co-stimulation to promote tumor immunity. *J Exp Med*. 2010; 207(10):2195–206. [PubMed: 20837698]
22. Cho HI, Celis E. Optimized peptide vaccines eliciting extensive CD8 T-cell responses with therapeutic antitumor effects. *Cancer Res*. 2009; 69(23):9012–9. [PubMed: 19903852]
23. Cho HI, Lee YR, Celis E. Interferon gamma limits the effectiveness of melanoma peptide vaccines. *Blood*. 2011; 117(1):135–44. [PubMed: 20889921]
24. Hochedlinger K, Jaenisch R. Monoclonal mice generated by nuclear transfer from mature B and T donor cells. *Nature*. 2002; 415(6875):1035–8. [PubMed: 11875572]
25. Frickel EM, Sahoo N, Hopp J, Gubbels MJ, Craver MP, Knoll LJ, et al. Parasite stage-specific recognition of endogenous *Toxoplasma gondii*-derived CD8+ T cell epitopes. *J Infect Dis*. 2008; 198(11):1625–33. [PubMed: 18922097]
26. Gredmark-Russ S, Cheung EJ, Isaacson MK, Ploegh HL, Grotenbreg GM. The CD8 T-cell response against murine gammaherpesvirus 68 is directed toward a broad repertoire of epitopes from both early and late antigens. *J Virol*. 2008; 82(24):12205–12. [PubMed: 18922872]
27. Grotenbreg GM, Roan NR, Guillen E, Meijers R, Wang JH, Bell GW, et al. Discovery of CD8+ T cell epitopes in *Chlamydia trachomatis* infection through use of caged class I MHC tetramers. *Proc Natl Acad Sci U S A*. 2008; 105(10):3831–6. [PubMed: 18245382]

28. Wilde S, Sommermeyer D, Leisegang M, Frankenberger B, Mosetter B, Uckert W, et al. Human antitumor CD8+ T cells producing Th1 polycytokines show superior antigen sensitivity and tumor recognition. *J Immunol.* 2012; 189(2):598–605. [PubMed: 22689880]
29. Laugel B, van den Berg HA, Gostick E, Cole DK, Wooldridge L, Boulter J, et al. Different T cell receptor affinity thresholds and CD8 coreceptor dependence govern cytotoxic T lymphocyte activation and tetramer binding properties. *J Biol Chem.* 2007; 282(33):23799–810. [PubMed: 17540778]
30. Azzam HS, Grinberg A, Lui K, Shen H, Shores EW, Love PE. CD5 expression is developmentally regulated by T cell receptor (TCR) signals and TCR avidity. *J Exp Med.* 1998; 188(12):2301–11. [PubMed: 9858516]
31. Rizzuto GA, Merghoub T, Hirschhorn-Cymerman D, Liu C, Lesokhin AM, Sahawneh D, et al. Self-antigen-specific CD8+ T cell precursor frequency determines the quality of the antitumor immune response. *J Exp Med.* 2009; 206(4):849–66. [PubMed: 19332877]
32. Woo SR, Turnis ME, Goldberg MV, Bankoti J, Selby M, Nirschl CJ, et al. Immune inhibitory molecules LAG-3 and PD-1 synergistically regulate T-cell function to promote tumoral immune escape. *Cancer Res.* 2012; 72(4):917–27. [PubMed: 22186141]
33. Wherry EJ, Ha SJ, Kaech SM, Haining WN, Sarkar S, Kalia V, et al. Molecular signature of CD8+ T cell exhaustion during chronic viral infection. *Immunity.* 2007; 27(4):670–84. [PubMed: 17950003]
34. Scholler J, Brady TL, Binder-Scholl G, Hwang WT, Plesa G, Hege KM, et al. Decade-long safety and function of retroviral-modified chimeric antigen receptor T cells. *Sci Transl Med.* 2012; 4(132):132ra53.
35. Lanitis E, Poussin M, Klattenhoff A, Song D, Sandaltzopoulos R, June C, et al. Chimeric Antigen Receptor T Cells with Dissociated Signaling Domains Exhibit Focused Antitumor Activity with Reduced Potential for Toxicity In Vivo. *Cancer Immunology Research.* 2013
36. Khan N, Cobbold M, Cummerson J, Moss PA. Persistent viral infection in humans can drive high frequency low-affinity T-cell expansions. *Immunology.* 2010; 131(4):537–548. [PubMed: 20722762]
37. Kalia V, Sarkar S, Ahmed R. CD8 T-cell memory differentiation during acute and chronic viral infections. *Adv Exp Med Biol.* 684:79–95. [PubMed: 20795542]
38. Sarkar S, Kalia V, Haining WN, Konieczny BT, Subramaniam S, Ahmed R. Functional and genomic profiling of effector CD8 T cell subsets with distinct memory fates. *J Exp Med.* 2008; 205(3):625–40. [PubMed: 18316415]
39. Sarkar S, Teichgraber V, Kalia V, Polley A, Masopust D, Harrington LE, et al. Strength of stimulus and clonal competition impact the rate of memory CD8 T cell differentiation. *J Immunol.* 2007; 179(10):6704–14. [PubMed: 17982060]
40. Feinerman O, Veiga J, Dorfman JR, Germain RN, Altan-Bonnet G. Variability and robustness in T cell activation from regulated heterogeneity in protein levels. *Science.* 2008; 321(5892):1081–4. [PubMed: 18719282]
41. Mackensen A, Meidenbauer N, Vogl S, Laumer M, Berger J, Andreesen R. Phase I study of adoptive T-cell therapy using antigen-specific CD8+ T cells for the treatment of patients with metastatic melanoma. *J Clin Oncol.* 2006; 24(31):5060–9. [PubMed: 17075125]
42. Yee C, Thompson JA, Byrd D, Riddell SR, Roche P, Celis E, et al. Adoptive T cell therapy using antigen-specific CD8+ T cell clones for the treatment of patients with metastatic melanoma: in vivo persistence, migration, and antitumor effect of transferred T cells. *Proc Natl Acad Sci U S A.* 2002; 99(25):16168–73. [PubMed: 12427970]
43. Yee C, Thompson JA, Roche P, Byrd DR, Lee PP, Piepkorn M, et al. Melanocyte destruction after antigen-specific immunotherapy of melanoma: direct evidence of t cell-mediated vitiligo. *J Exp Med.* 2000; 192(11):1637–44. [PubMed: 11104805]
44. Bos R, Marquardt KL, Cheung J, Sherman LA. Functional differences between low- and high-affinity CD8(+) T cells in the tumor environment. *Oncoimmunology.* 2012; 1(8):1239–47. [PubMed: 23243587]

45. Lyman MA, Nugent CT, Marquardt KL, Biggs JA, Pamer EG, Sherman LA. The fate of low affinity tumor-specific CD8+ T cells in tumor-bearing mice. *J Immunol.* 2005; 174(5):2563–72. [PubMed: 15728462]
46. Janicki CN, Jenkinson SR, Williams NA, Morgan DJ. Loss of CTL function among high-avidity tumor-specific CD8+ T cells following tumor infiltration. *Cancer Res.* 2008; 68(8):2993–3000. [PubMed: 18413769]
47. Jordan KR, Buhrman JD, Sprague J, Moore BL, Gao D, Kappler JW, et al. TCR hypervariable regions expressed by T cells that respond to effective tumor vaccines. *Cancer Immunol Immunother.* 2012; 61(10):1627–38. [PubMed: 22350070]
48. Chervin AS, Stone JD, Soto CM, Engels B, Schreiber H, Roy EJ, et al. Design of T-cell receptor libraries with diverse binding properties to examine adoptive T-cell responses. *Gene Ther.* 2012
49. Irving M, Zoete V, Hebeisen M, Schmid D, Baumgartner P, Guillaume P, et al. Interplay between T cell receptor binding kinetics and the level of cognate peptide presented by major histocompatibility complexes governs CD8+ T cell responsiveness. *J Biol Chem.* 2012; 287(27):23068–78. [PubMed: 22549784]
50. Schmid DA, Irving MB, Posevitz V, Hebeisen M, Posevitz-Fejfar A, Sarria JC, et al. Evidence for a TCR affinity threshold delimiting maximal CD8 T cell function. *J Immunol.* 2010; 184(9):4936–46. [PubMed: 20351194]
51. McMahan RH, McWilliams JA, Jordan KR, Dow SW, Wilson DB, Slansky JE. Relating TCR-peptide-MHC affinity to immunogenicity for the design of tumor vaccines. *J Clin Invest.* 2006; 116(9):2543–51. [PubMed: 16932807]
52. O’Sullivan JA, Zloza A, Kohlhapp FJ, Moore TV, Lacey AT, Dulin NO, et al. Priming with very low-affinity peptide ligands gives rise to CD8(+) T-cell effectors with enhanced function but with greater susceptibility to transforming growth factor (TGF)β-mediated suppression. *Cancer Immunol Immunother.* 2011; 60(11):1543–51. [PubMed: 21681376]
53. Ohlfest JR, Andersen BM, Litterman AJ, Xia J, Pennell CA, Swier LE, et al. Vaccine Injection Site Matters: Qualitative and Quantitative Defects in CD8 T Cells Primed as a Function of Proximity to the Tumor in a Murine Glioma Model. *J Immunol.* 2012; 190(2):613–620. [PubMed: 23248259]
54. Tabbekh M, Franciszkiwicz K, Haouas H, Lecluse Y, Benihoud K, Raman C, et al. Rescue of tumor-infiltrating lymphocytes from activation-induced cell death enhances the antitumor CTL response in CD5-deficient mice. *J Immunol.* 2011; 187(1):102–9. [PubMed: 21622855]
55. Kim EY, Teh SJ, Yang J, Chow MT, Teh HS. TNFR2-deficient memory CD8 T cells provide superior protection against tumor cell growth. *J Immunol.* 2009; 183(10):6051–7. [PubMed: 19841176]
56. Vanneman M, Dranoff G. Combining immunotherapy and targeted therapies in cancer treatment. *Nat Rev Cancer.* 2012; 12(4):237–51. [PubMed: 22437869]

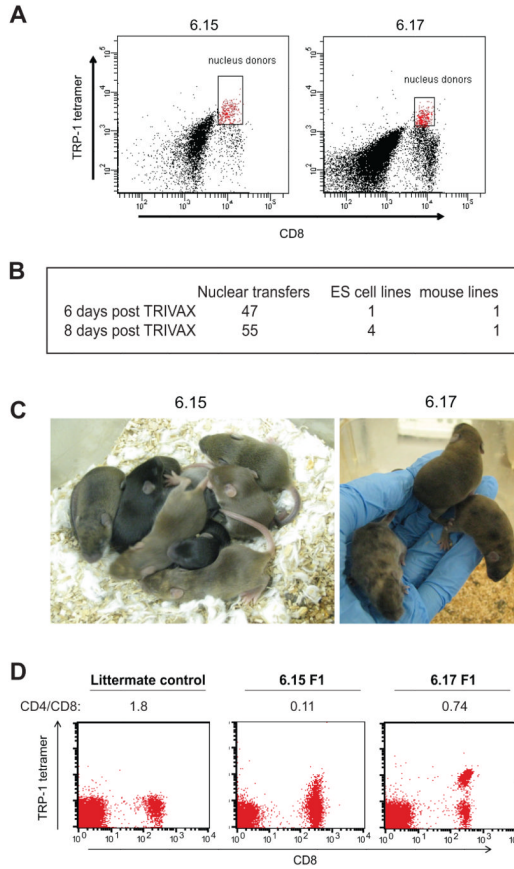


Figure 1. TRP1 TN mice were derived from TRP1-specific CD8 T cells. A) C57BL/6x129 F1 agouti male mice were immunized with TRIVAX (palmitoylated TAPDNLGYM 10 μ g/mouse, anti-CD40 30 μ g/mouse and poly-IC 15 μ g/mouse) intravenously. Splenocytes were harvested 6 or 8 days post-immunization and stained with anti-CD8 and TRP1 tetramer. Gated cells were sorted by FACS and used as nucleus donors for SCNT. B) Success rate of nuclear transfer. C) ES cell lines 6.15 and 6.17 were injected into wild type blastocysts to generate chimeric mice as shown. Germline transmission was achieved by crossing chimeras to C57BL/6 females. D) Peripheral blood mononuclear cells were harvested from germline transmitted 6.15 or 6.17 mice and stained with TRP1 tetramer, anti-CD4 and anti-CD8. The calculated CD4:CD8 ratio is shown below each plot. Note the lower intensity tetramer staining in the 6.15 mouse, representative of more than 100 mice analyzed.

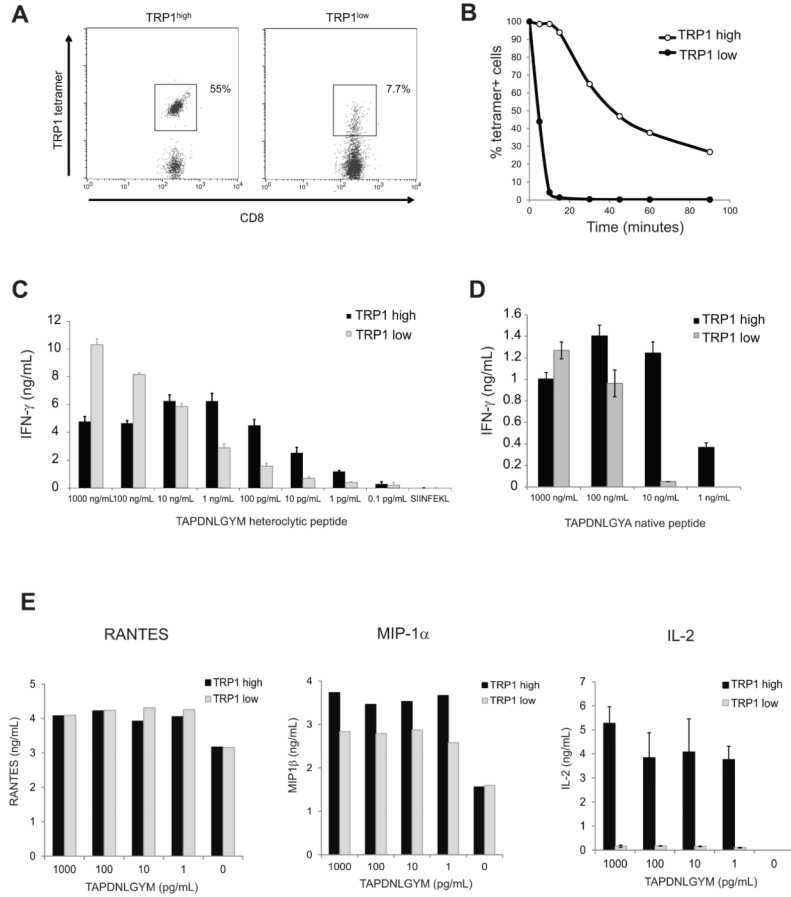


Figure 2. TRP1 TN lines differ in TCR affinity. A) Splenocytes from TRP1^{low} (6.15) and TRP1^{high} (6.17) TN mice were stained with TRP1 tetramer to saturation, washed, and incubated at room temperature for various times prior to fixation and analysis by flow cytometry. Time 0 is shown. B) Percent tetramer+ cells as defined by the gates shown in A were calculated for each time point and normalized to Time 0. Representative of 3 independent experiments. C) CD8 T cells isolated from TRP1^{low} or TRP1^{high} mice were cocultured with BMDCs pulsed with TAPDNLGYM at the indicated concentrations. IFN- γ was measured by ELISA of 48 hr culture supernatants. Representative of 5 independent experiments. D) CD8 T cells were cocultured as in (C) using BMDCs pulsed with the native TRP1 peptide (TAPDNLGYA). Representative of 3 independent experiments. E) CD8 T cells were cultured as in (C). RANTES and MIP-1 α were analyzed by cytokine bead array using 24 hr culture supernatants; IL-2 was measured by ELISA of the same supernatants. Representative of 3 independent experiments.

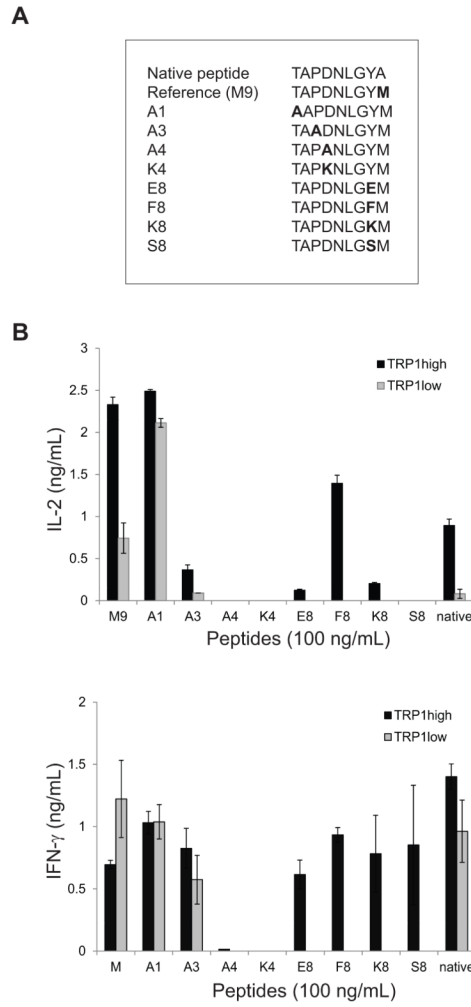


Figure 3. Fine specificity mapping of TRP TN TCR specificities. A) An altered peptide library (as shown) was generated by substitution of non MHC contact residues. B) CD8 T cells isolated from TRP1^{high} or TRP1^{low} mice were cocultured with BMDCs pulsed with the indicated peptides at 100 ng/mL. IL-2 was measured by ELISA of 24hr culture supernatants. IFN- γ was measured by ELISA of 72hr culture supernatants. Representative of 2 independent experiments. Error bars are SD of triplicate samples.

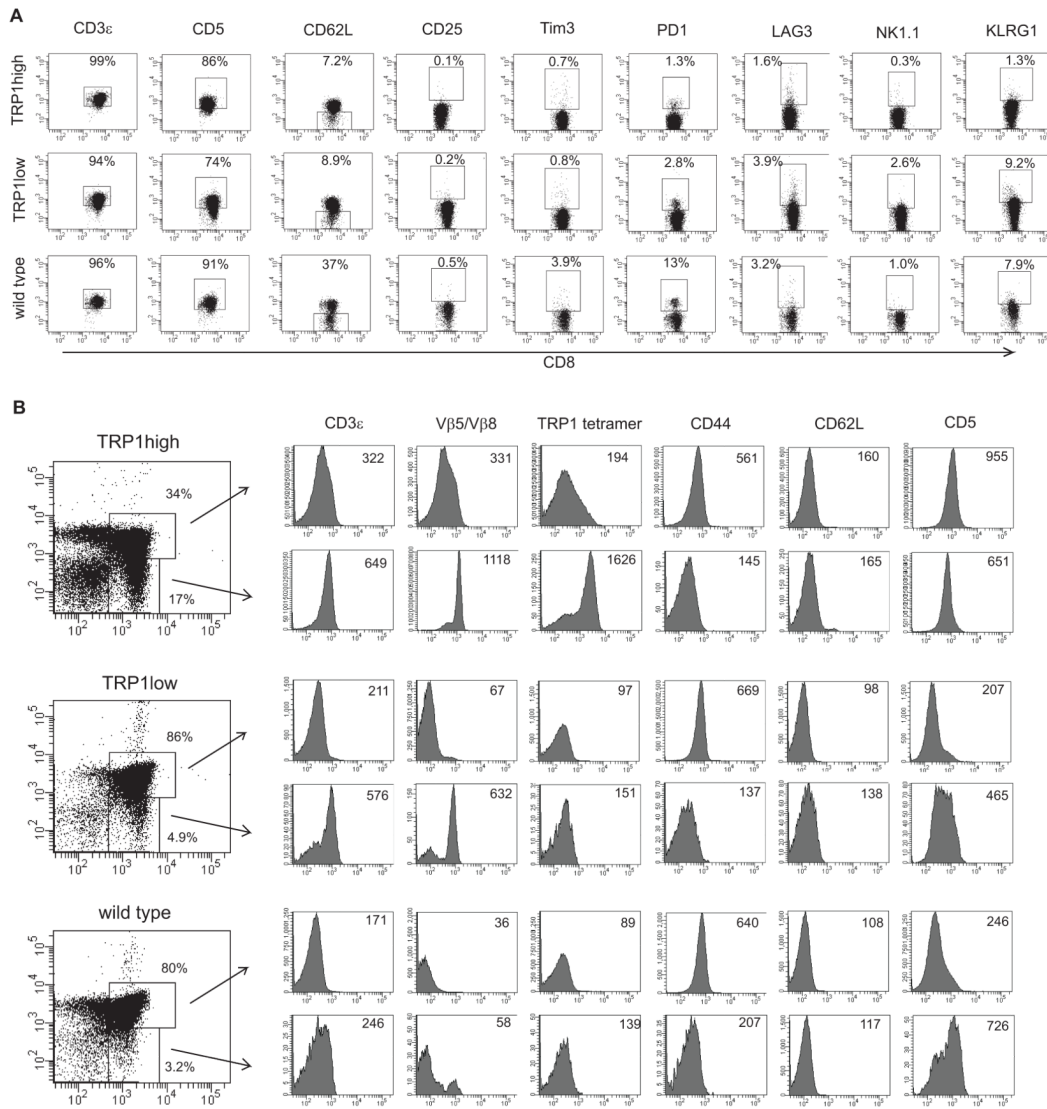


Figure 4.

Surface profiling and thymic development of TRP1 TN CD8 cells. A) Pooled spleen and lymph node cells from 6 week old male TRP1^{high}, TRP1^{low} and C57BL/6 mice were stained with the indicated antibodies. Plots shown are gated on CD8⁺ cells. B) Thymocytes from 6 week old male TRP1^{high}, TRP1^{low} and C57BL/6 mice were stained with the indicated antibodies. Histogram plots are gated on CD4⁺CD8⁺ double positive cells (top rows) or on CD8⁺ single positive cells (bottom rows). Numbers indicate median fluorescent intensities of histograms. TRP1^{low} cells show negligible tetramer staining. To confirm genotype, naive CD8 T cells from the same mice were stimulated with APCs and TRP1 A1 peptide in tissue culture, and activation was assessed by CD69 expression. %CD69⁺: TRP1^{high} = 81% (no peptide = 0.5%); TRP1^{low} = 35% (no peptide = 0.3%).

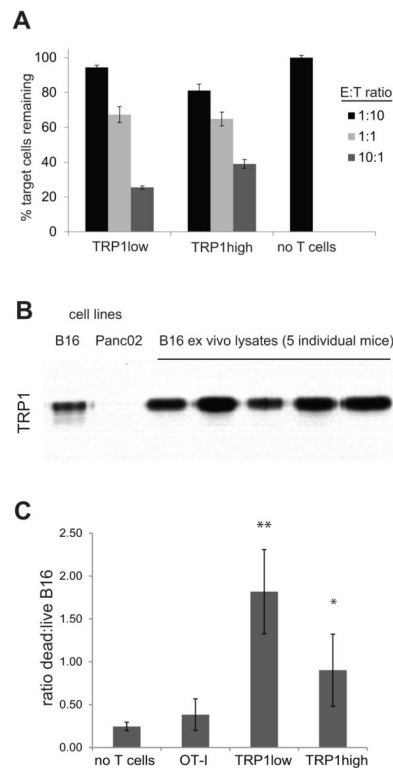


Figure 5.

TRP1 TN CD8 T cells are tumoricidal in vitro. A) CD8⁺ T cells were harvested from the indicated mice and cultured for 8 days with anti-CD3/CD28 beads and IL-2 (20 U/mL). Activated T cells were washed, counted, and aliquoted into a 96 well round bottom plate at 50,000 T cells per well. B cells were harvested from a wildtype or MHCII-GFP mouse. GFP⁺ B cells were incubated with 100uM TRP1 A1 peptide for 2 hours, washed twice, counted and mixed with non-GFP cells at a 1:1 ratio. This B cell mixture was then added to the plated T cells at the indicated ratios where E = effector T cells and T = total pooled B cells. After 48 hours of coculture, the cells were stained with anti-CD19 and the viability dye 7-AAD. B) Lysates were prepared from cultured B16 or Panc02 cells, and from B16 tumors >1cm in diameter resected from tumor-bearing mice. Immunoblotting shows TRP1 protein expression. C) CD8 T cells were cultured for 18 hours with BMDCs and their cognate peptide to induce activated. Peptide activated CD8 T cells were counted, washed, and seeded with B16 cells in Matrigel at 10:1 ratio. 3D cultures were incubated for 4 days; cells were reisolated and stained with anti-CD8 and the viability dye 7-AAD. B16 cells were gated by FSC/SSC profile of CD8⁻ cells. The ratio of 7AAD⁺:7AAD⁻ cells is shown. Representative of 2 independent experiments. Error bars are SD. * p=0.026, ** p=0.005 vs. OT-I.

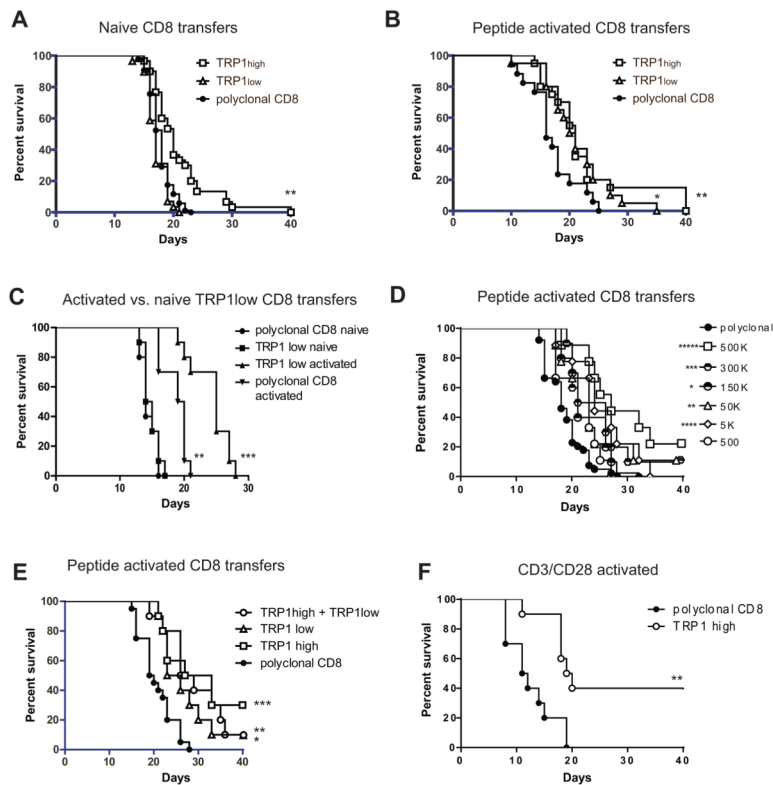


Figure 6.

TRP1 CD8 T cells delay tumor growth in vivo. A) Naïve CD8 T cells were harvested from TRP1^{high}, TRP1^{low} or wild type mice and transferred at 3 million cells per mouse into female C57BL/6 recipients. On the same day, 50,000 B16 tumor cells were inoculated subcutaneously. Tumor volume was measured over time, and mice were euthanized when tumor size reached 2 cm³. n=30 mice per group, pooled from 3 independent experiments. **p=0.0001 vs. polyclonal CD8. B) CD8 T cells were harvested from TRP1 TN mice and cultured with BMDCs pulsed with TRP1 heteroclytic peptide for 18 hours. CD8 cells were harvested, washed, counted and transferred to recipient C57BL/6 mice at 3 million cells per mouse one day after inoculation with 50,000 B16 cells. n=30 mice per group, pooled from 3 independent experiments. *p=0.0119, **p=0.0161 vs. polyclonal CD8. C) CD8 T cells were harvested from TRP1^{low} or C57BL/6 donor mice and transferred into recipients either directly (naïve) or after 18 hours of culture with peptide-pulsed BMDCs (activated). Recipient mice were inoculated with B16 cells on the same day as naïve cell transfer, or one day prior to activated cell transfer. **p=0.001 vs polyclonal CD8 naïve, ***p=0.0005 vs, polyclonal CD8 activated. D) CD8 T cells were harvested from TRP1 TN mice and cultured with BMDCs pulsed with TRP1 heteroclytic peptide for 18 hours. CD8 cells were harvested, washed, counted and transferred to recipient C57BL/6 mice at the indicated number of cells per mouse one day after inoculation with 50,000 B16 cells. n=10 mice per group. *p=0.0361, **p=0.012, ***p=.0045, ****p=0.0011, *****p<0.0001 vs. polyclonal CD8. E) CD8 T cells were harvested from TRP1 TN mice and cultured with BMDCs pulsed with TRP1 heteroclytic peptide for 18 hours. CD8 cells were harvested, washed, counted and transferred to recipient C57BL/6 mice at 300,000 cells per mouse one day after inoculation with 50,000 B16 cells. n=10 mice per group. *p=0.0047, **p=0.0008, *** p=0.0004 vs. polyclonal CD8. F) CD8 T cells were harvested from C57BL/6 mice or TRP1^{high} mice and cultured for 5 days with anti-CD3/CD28 coated beads. CD8 cells were harvested, washed,

counted and transferred into C57BL/6 recipient mice at 300,000 cells per mouse one day after inoculation with 50,000 B16 cells. ** $p=0.0021$.

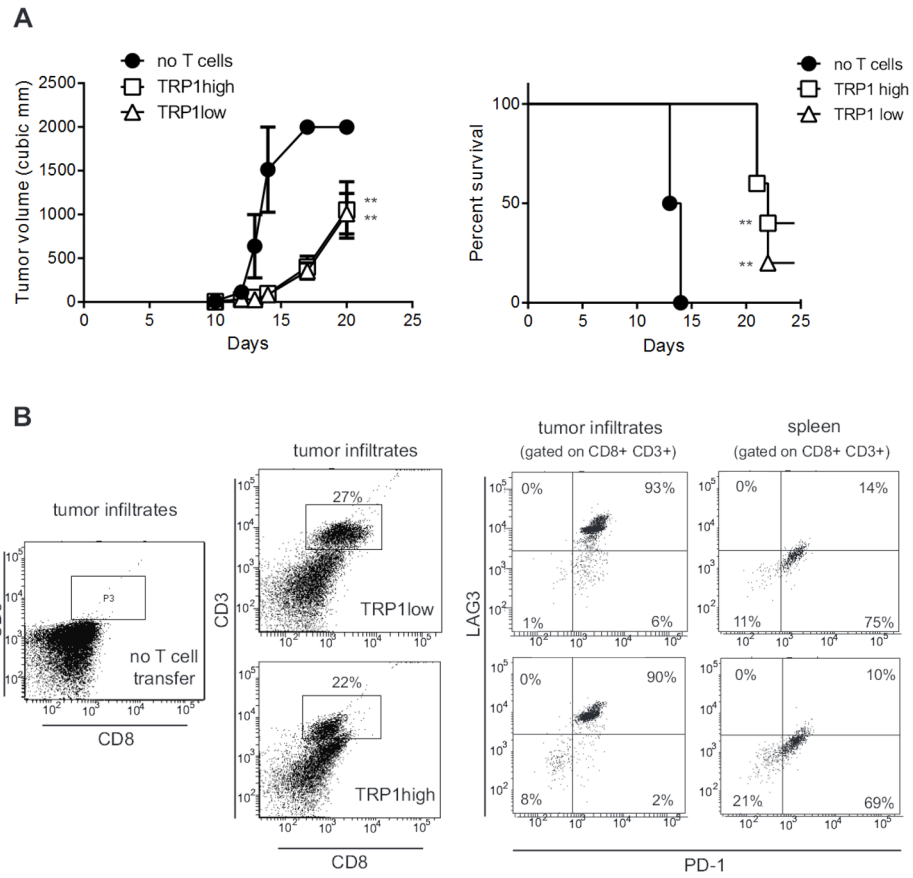


Figure 7. TRP1 TN cells migrating to the tumor show an exhausted phenotype. A) RAG2^{-/-} mice were inoculated with 100,000 B16 cells one day prior to transfer of naïve CD8+ T cells from TRP1^{high} or TRP1^{low} TN mice. Tumor volume was measured over time. **p=0.001. Representative of 3 independent experiments. B) End stage tumors from mice in A) were harvested, digested with collagenase and tumor infiltrating lymphocytes were analyzed by flow cytometry after staining with the indicated antibodies. n=5 mice per group.